Electronic Supplementary Material (ESI) for Nanoscale.
This journal is © The Royal Society of Chemistry 2024

Gallic acid loaded HFZIF-8 for tumor targeted delivery and thermal catalytic therapy

Xing Yang,[ac] Chunsheng Li,[a] Shuang Liu,[a] Yunlong Li,[a] Xinyu Zhang,[a] Qiang Wang,[a] Jin Ye,[a] Yong Lu,[acd] Yujie Fu,[b] and Jiating Xu*[abc]

[a] Key Laboratory of Forest Plant Ecology, Ministry of Education, College of Chemistry, Chemical Engineering and Resource Utilization, Northeast Forestry University, Harbin 150040, P. R. China

[b] College of Forestry, Beijing Forestry University, Beijing 100083, P.R. China

[c] Heilongjiang Provincial Key Laboratory of Ecological Utilization of Forestry-Based Active Substances, Northeast Forestry University, Harbin, 150040, P. R. China

[d] School of Laboratory Medicine, Wannan Medical College, Wuhu, Anhui 241002, P.R. China

1. Materials

Ferrous sulfate ($FeSO_4$•$7H_2O$) was purchased from Aladdin. Hydrochloric acid (HCl) was purchased from Sinopharm Chemical Reagent Co., China. Methanol (CH_3OH), ethanol (CH_3CH_2OH), 2-methylimidazole (2-MeIM), and cetyl trimethyl ammonium bromide (CTAB) were purchased from Fuyu Fine Chemical Co., Ltd. Sodium hydroxide (NaOH) was purchased from Guangfu (China), tannic acid (TA)， hyaluronic acid (HA), and gallic acid (GA) were purchased from Rhawn. Phosphate buffer solution (PBS) (pH 7.0) and PBS (pH 5.6) were purchased from Beyotime Biotechnology Co., Ltd. Hydrogen peroxide (H_2O_2), fluorescein isothiocyanate (FITC), 1,3-Diphenylisobenzofuran (DPBF), glutathione (GSH), 2,7-Dichlorodihydrofluorescein diacetate (DCFH-DA), methyl orange (MO), 5,5-dimethyl-1-pyrrolineN-oxide (DMPO), 4,6-diamidino-2-phenylindole (DAPI), zinc nitrate hexahydrate ($ZnNO_3$•$6H_2O$) and 3-4,5-dimethylthiazol-2-yl-2,5-diphenyl tetrazolium bromide (MTT) were purchased from Sigma-Aldrich. All the reagents were analytical grade without further purification. Calcein-acetoxymethyl ester (calcein-AM) and propidium iodide (PI) were acquired from Beijing Solarbio Science & Technology Co., Ltd.

2. Characterization

The X-ray diffraction (XRD) patterns of the samples were recorded on a powder X-ray diffractometer with radiation (1.5419 Å) from 5° to 80° at a scanning rate of 7°/min. The transmission electron microscopy (TEM) graphs were obtained from JEM-2100. The scanning electron microscope (SEM) graphs were obtained from JSM-7500F. The infrared spectra were measured using a Fourier-transform infrared (FTIR) spectrometer Spectrum 400

(PerkinElmer) within wavenumber range of 4000-500 cm^{-1}. Ultraviolet-visible (UV-vis) absorption spectra were tested on a Classic Dual Beam UV-vis Spectrophotometer Cary100, N_2 adsorption-desorption isotherms and pore-size distributions were tested on BELSORP-max (Japan). *In vitro* elemental analyses for the degradation products of HFZIF-8/GA@HA were conducted on inductively coupled plasma-optical emission spectrometry (ICP-OES).

3. The blood routines and serum biochemistry assay

Ten healthy Kunming female mice were divided into two groups (n = 5). One was used as a control group, and another group was injected with 50 μL PBS solution containing 500 μg/mL of HFZIF-8/GA@HA. After 14 days, the blood samples were obtained by extracting eyeball blood to test the blood routines and serum biochemistry indicators.

4. *In vitro* degradation experiment

HFZIF-8/GA@HA was added into two different solutions including PBS (pH 6.5), PBS (pH 7.0). Then the above solutions were sonicated for 3 min and elemental analysis of these samples was performed by ICP-OES after shaking on a shaker for different time durations.

5. GA loading rate

After the mixing and stirring process of GA and HFZIF-8 is finished, the mixed solution was centrifugally separated at 8000 rpm for 3 times, and then the supernatant solution was collected for UV-vis analysis. The loading capacity and concentration of GA in the solution were determined by UV-vis at the wavelength of 259 nm. According to the standard curve $A_{259nm} = 41.269B + 0.146$, the unloaded GA can be calculate: $IE\% = (M_1 - M_2)\ M_1 \times 100\%$ (M_1 is total drug and M_2 is drug in supernatant), and the loading rate of GA was also obtained.

6. Detection of ·OH

200 μL of methol solution containing 1 mg of HFZIF-8/GA@HA, 200 μL of NaCl solution (50 mM), 300 μL of GSH solution (10 mM) and 800 μL of $NaHCO_3$ buffer solution were mixed and shaken for 15 min. After that, 100 μL of H_2O_2 (20 mM) and 500 μL of MO (100 μg/mL) were mixed and added in above solution, co-culturing for 15 min at 37 °C. Finally, the absorbance of MO with different treatment were detected by a UV-vis absorption spectrum.

7. The cellular uptake evaluation of the HFZIF-8/GA@HA

HeLa cells were inoculated into a 6-well plate and incubated for 24 h to obtain the monolayer of cells. Then, the FITC-modified HFZIF-8/GA@HA (1 mL, 0.5 mg/mL) was transferred in 6-well plate and cultured for 0.5 h. Afterwards, the cells were rinsed three times with saline, and then DAPI was joined in each well to dye the cell nucleus for 15 min. Subsequently, HeLa cells were fixed with glutaraldehyde. At last, the cells were further rinsed several times by saline for observing the fluorescence images.

8. *In vitro* cytotoxicity detection

The monolayer Hela cells were inoculated in a 96-well plate and incubated overnight in humid condition (37 °C, 5% CO_2). 1 mg of HFZIF-8/GA@HA was diluted by culture medium to obtain these solutions with concentrations of 0, 15.6, 31.3, 62.5, 125, 250 and 500 μg/mL. The HZIF-8@HA (1 mg) was diluted by the same method for the subsequent use. 12 wells of cells were untreated as a blank group. Then, other wells were divided into four groups of NIR (1.0 W/cm^2), HZIF-8@HA, HFZIF-8/GA@HA and HFZIF-8/GA@HA plus

NIR, respectively. Subsequently, the culture solution was removed, and 20 μL of MTT solution was added to the 96-well plate and cultured for a period. At last, 160 μL of dimethyl sulfoxide was injected into these wells for the test of the microplate reader.

9. Staining of living and dead cells

Calcein-AM/PI staining method was employed to further evaluate the cytotoxicity of as-synthesized materials. HeLa cells were treated with PBS, 1064 nm laser irradiation, HFZIF-8@HA incubation, HFZIF-8/GA@HA incubation, HFZIF-8/GA@HA incubation plus 1064 nm laser (1.0 W/cm^2, 10 min), respectively. Then, the cells were stained with a mixture of calcein-AM (2 μM) and PI (4.5 μM) for 30 min. Finally, the stained-cells were then observed using CLSM after being rinsed three times with PBS solution.

10. Intracellular ROS detection

The HeLa cells that have just been passaged were incubated for 24 h. Then, they were added into a 6-well plate. One well of the plate was left untreated as a blank group, then the other four wells were treated with NIR irradiation (1.0 W/cm^2), HZIF-8@HA, HFZIF-8/GA@HA and HFZIF-8/GA@HA plus NIR irradiation, respectively. Afterwards, 1 mL of DCFH-DA was added into each well and cultured for another 15 min, rinsing three times with saline. The corresponding fluorescence pictures were observed with CLSM.

11. Biological transmission electron microscopy (Bio-TEM) tests

The HeLa cells were incubated with a DMEM medium containing 5% CO_2 at 37 °C for 24 h, and then were incubated with 1 mL DMEM medium containing HFZIF-8/GA@HA (200

μg/mL) for 1 h and 12 h. Then, the cells were washed for three times with PBS. Finally, Bio-TEM was used to observe the TEM images of these cells.

12. Flow cytometric analysis of apoptosis

Apoptosis was analyzed using the staining method of Annexin V-FITC/PI. Cells were treated with control, 1064 nm laser, HZIF-8@HA, HFZIF-8/GA@HA, HFZIF-8/GA@HA plus laser (1.0 W/cm^2, 10 min) and incubated for 12 h, respectively. Then, cells were harvested with trypsin, washed twice with PBS, and resuspended in 195 μL of binding solution, followed by the incubation with the 5 μL of Annexin V-FITC and 10 μL of PI under a dark condition for 15 min. Finally, staining cells were detected by flow cytometer.

13. Calculation of photothermal conversion efficacy

Photothermal conversion efficacy of the HFZIF-8/GA was calculated according to the temperature change of the PBS (pH 6.5) solution of HFZIF-8/GA as a function of time under continuous irradiation of a 1064 nm laser (1.0 W/cm^2) for 600 s until the solution reached a steady-state temperature. The photothermal conversion efficiency (η) can be calculated according to following Equation (1):

$$\eta = \frac{hS(T_{max} - T_{surr}) - Q_{dis}}{I(1 - 10^{-A1064})} \quad (1)$$

Where, h represents the heat transfer coefficient, S is the surface area of the container, T_{max} represents the maximum steady-state temperature (43.6 °C), T_{surr} is the ambient temperature of the environment (22.3 °C), Q_{dis} represents the heat dissipation from the light absorbed by the solvent and the quartz sample cell, I is the incident laser power (1.0 W/cm^2),

and A1064 is the absorbance of the sample at 1064 nm (0.186). The value of hS is derived from Equation (2-4):

$$\tau = \frac{M_D C_D}{hS} \quad (2)$$

$$\tau = \frac{-Ln(\theta)}{t} \quad (3)$$

$$\theta = \frac{T - T_{surr}}{T_{max} - T_{surr}} \quad (4)$$

Where τ is the time constant of HFZIF-8/GA aqueous dispersion for heat transfer of the system. M_D and C_D represent the mass (1.0 g) and heat capacity (4.2 J/g) of the deionized water used to disperse the HFZIF-8/GA, respectively. Additionally, *T* can denote the real-time temperature in the cooling period. As a result, τ was determined to be 261.51. While Q_{dis} can represent the heat dissipation from the light absorbed by the water and the quartz sample cell, so Q_{dis} was calculated according to Equation (5):

$$Q_{dis} = \frac{M_D C_D (T_{\max(water)} - T_{surr})}{\tau_{(water)}} \quad (5)$$

Where $T_{max(water)}$ is 28.7 °C, τ (water) was determined to be τ = 433.5. According to the obtained data and Equation (1), the photothermal conversion efficacy of the HFZIF-8/GA.

13. Antitumor study

Female Kunming mice were purchased from Second Affiliated Hospital of Harbin Medical University (Harbin, China) and all animal experiments were approved by the Ethics Committee of the Second Affiliated Hospital of Harbin Medical University. The cervical carcinoma (U14) tumors were injected in the back of each female mouse (28-34 g). When the tumor size grown to 150-180 mm^3, tumor-bearing mice were divided into five groups in a completely randomized manner, and treated with saline injection Laser irradiation (1.0

W/cm^2), HZIF-8@HA injection, HFZIF-8/GA@HA injection and HFZIF-8/GA@HA injection plus 1064 nm laser irradiation. The HZIF-8@HA and HFZIF-8/GA@HA were injected intravenously with a concentration of 500 μg/mL. In addition, the 1064 nm laser (10 min, 5 min break after 5 min irradiation) was used for irradiating tumors at 24 h post-injection of HFZIF-8/GA@HA. The tumor sizes were estimated with a rule every two days and calculated by the formula: (width × width × length)/2. Furthermore, each mouse was weighed every two days and the data was recorded. After 14 days, these mice were euthanized. Then the main organs of the tumor-bearing mice, such as heart, liver, spleen, lung, kidney, and tumor tissue were dissected from the body. Subsequently, the tumor weight of each mouse was obtained by an electronic analytical balance. Finally, the tumors and these organs were sectioned and stained with hematoxylin-eosin (H&E) and Ki67.

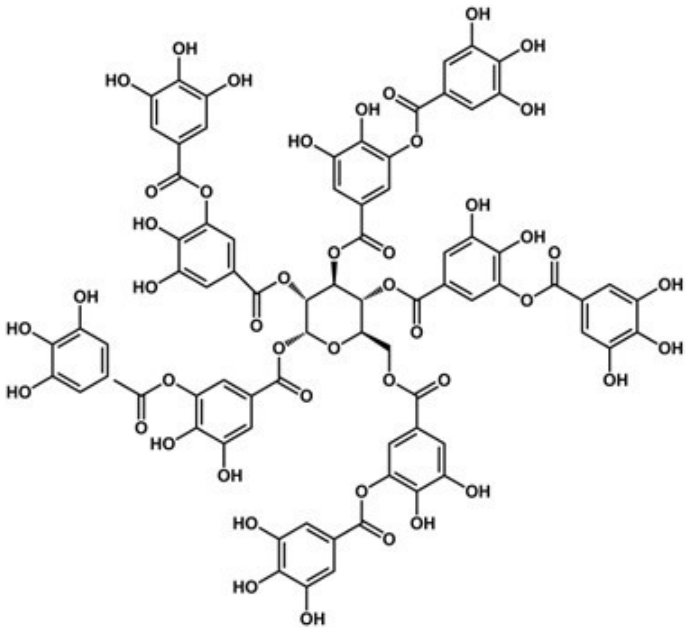

Fig. S1 The structural formula of TA.

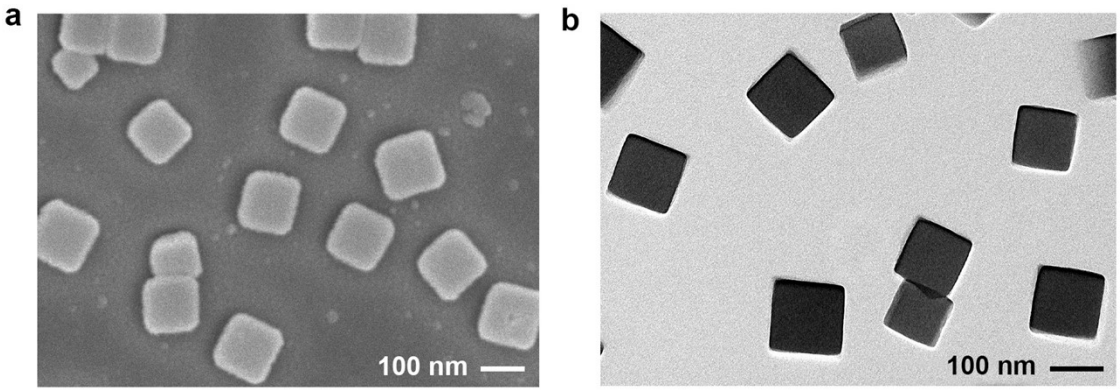

Fig. S2 SEM (a) and TEM (b) images of ZIF-8.

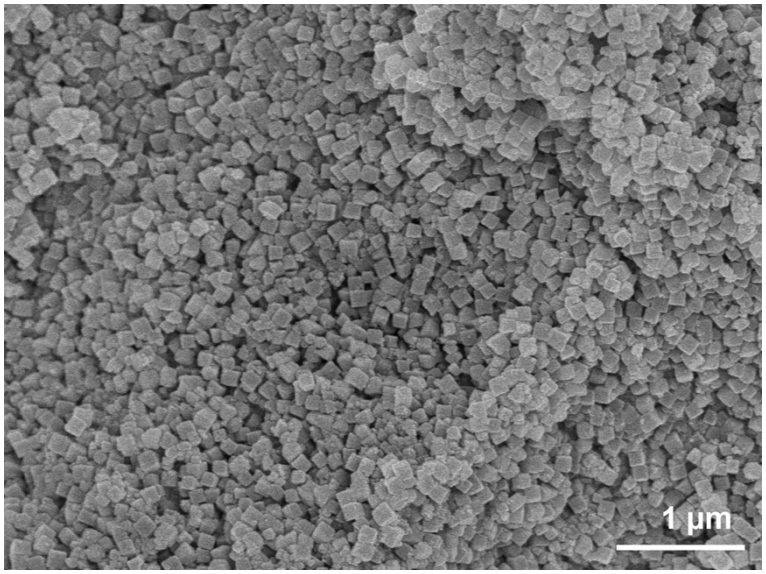

Fig. S3 SEM image of the Fe-doped ZIF-8.

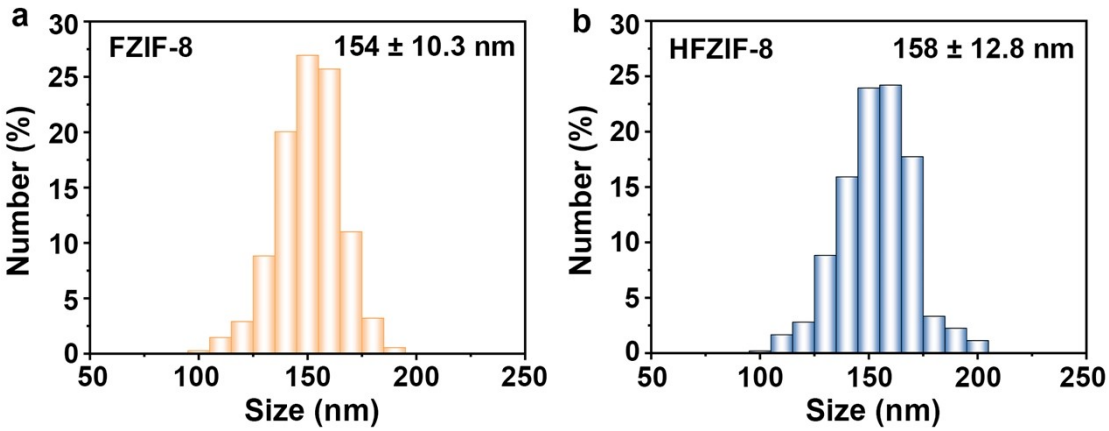

Fig. S4 The hydrodynamic diameters of FZIF-8 (a) and HFZIF-8 (b).

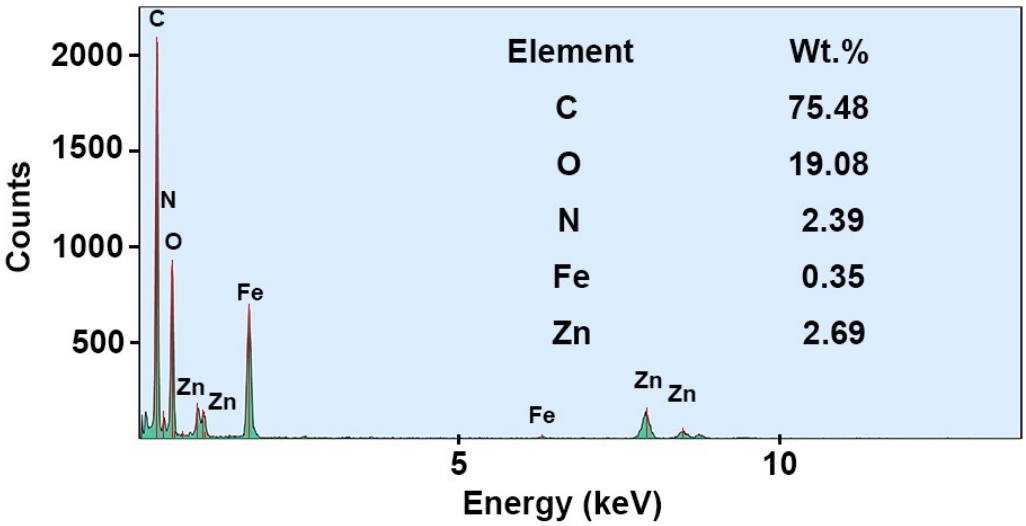

Fig. S5 EDS spectrum of the HFZIF-8.

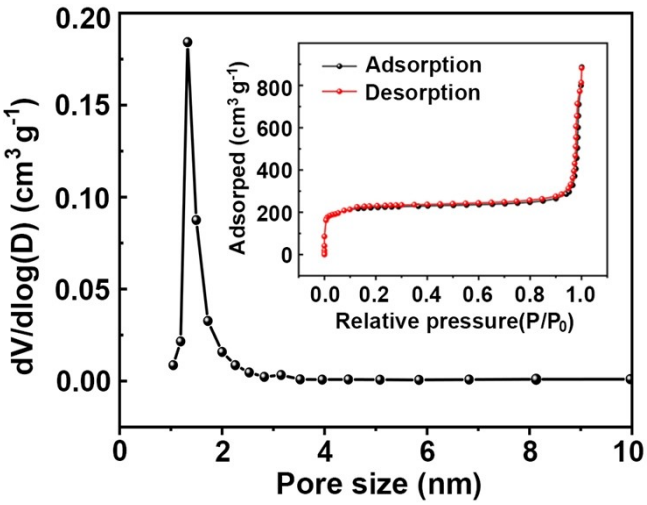

Fig. S6 Nitrogen sorption isotherms and BJH pore size distribution of the Fe-doped ZIF-8.

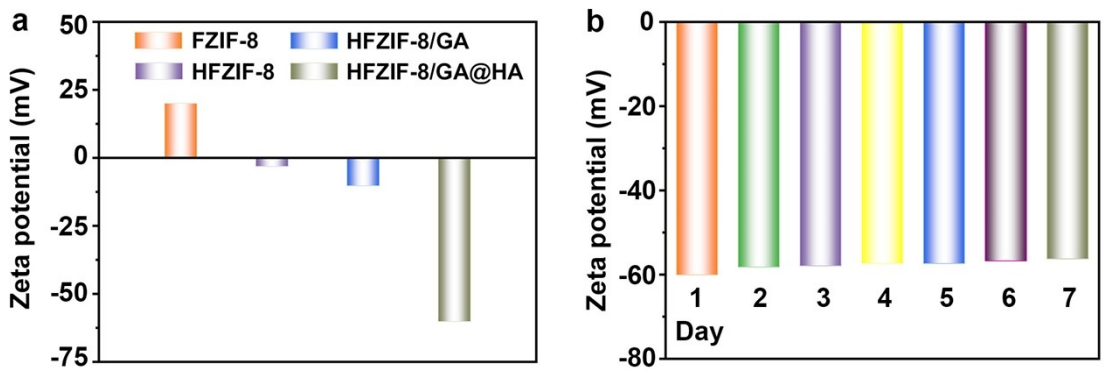

Fig. S7 Zeta potentials of FZIF-8, HFZIF-8, HFZIF-8/GA and HFZIF-8/GA@HA (a). Zeta potentials of HFZIF-8/GA@HA in a neutral environment during 7 days (b).

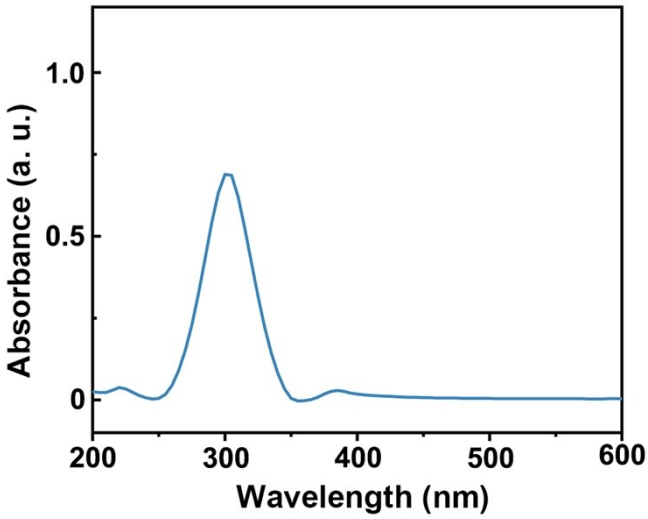

Fig. S8 The UV-vis absorption spectrum of the supernatant for HA modification reaction.

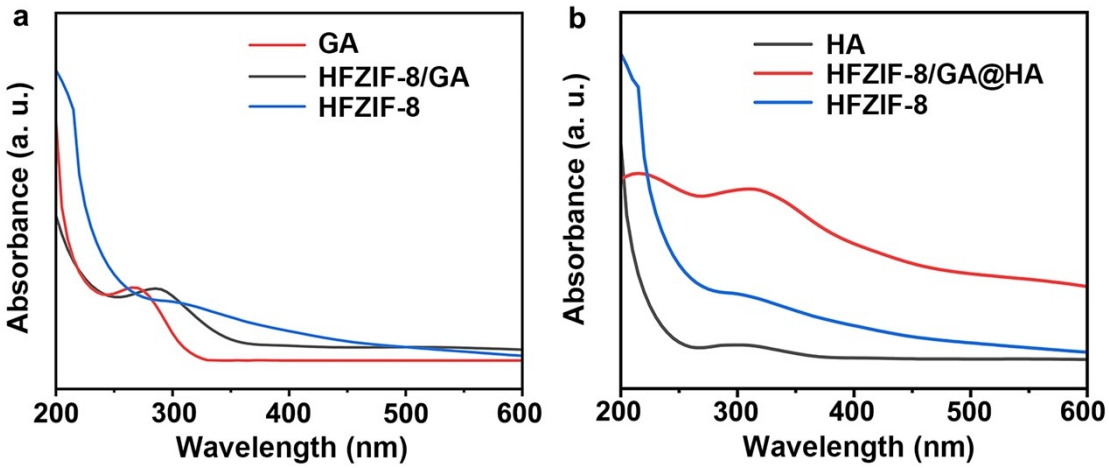

Fig. S9 The UV-vis absorption spectra of the HFZIF-8, HFZIF-8/GA and GA (a). The UV-vis absorption spectra of the HFZIF-8, HFZIF-8/GA@HA and HA (b).

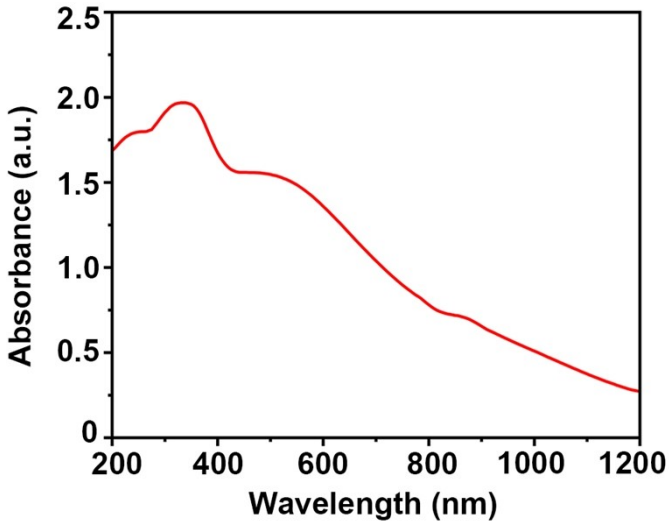

Fig. S10 The UV-vis DRS absorption spectrum of the HFZIF-8/GA.

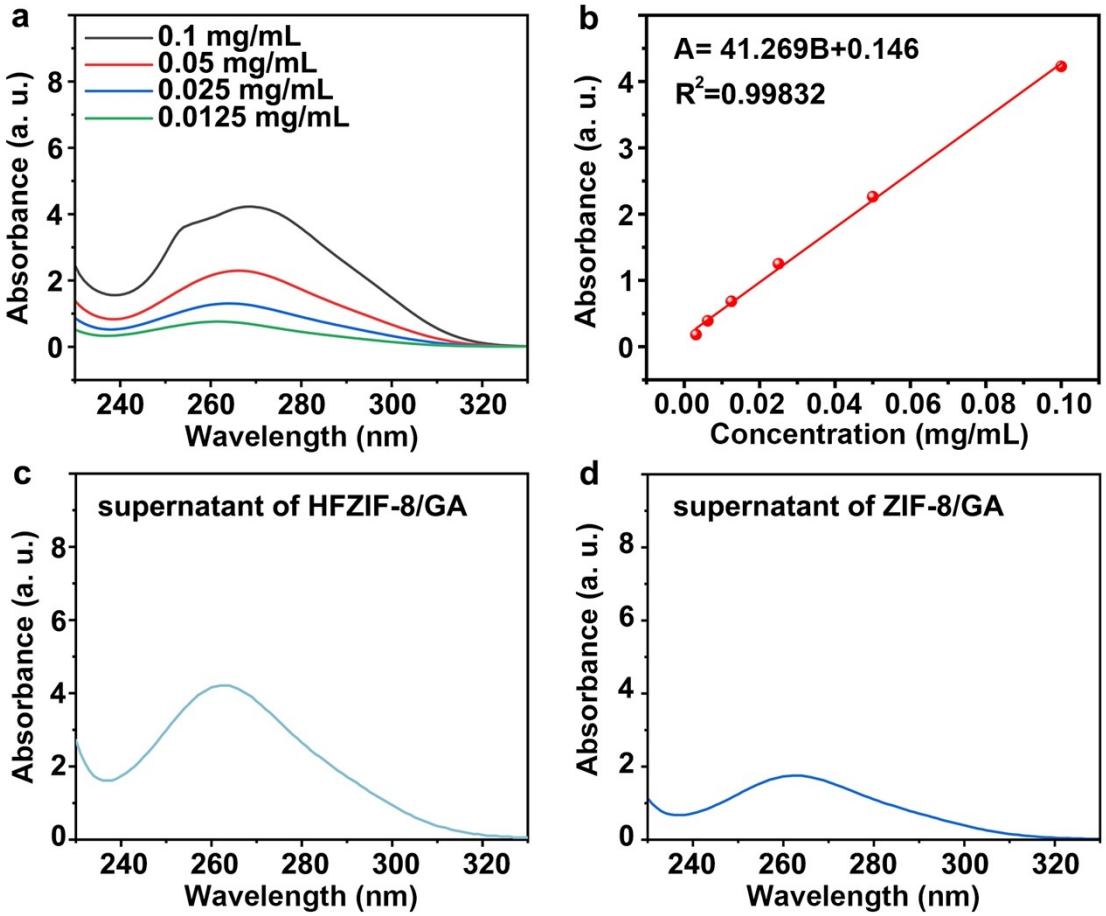

Fig. S11 UV-vis absorption spectra (a) and corresponding linear relation (b) of GA with different concentrations, and the absorption spectra of GA in HFZIF-8/GA (c) and ZIF-8/GA (d).

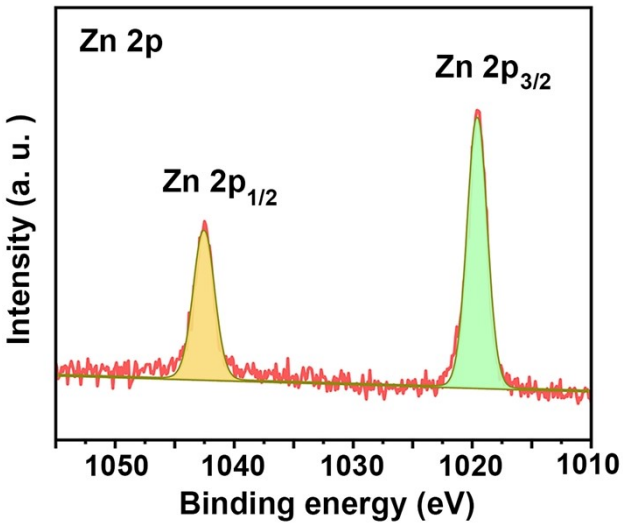

Fig. S12 The high-resolution XPS spectrum of Zn 2p in HFZIF-8.

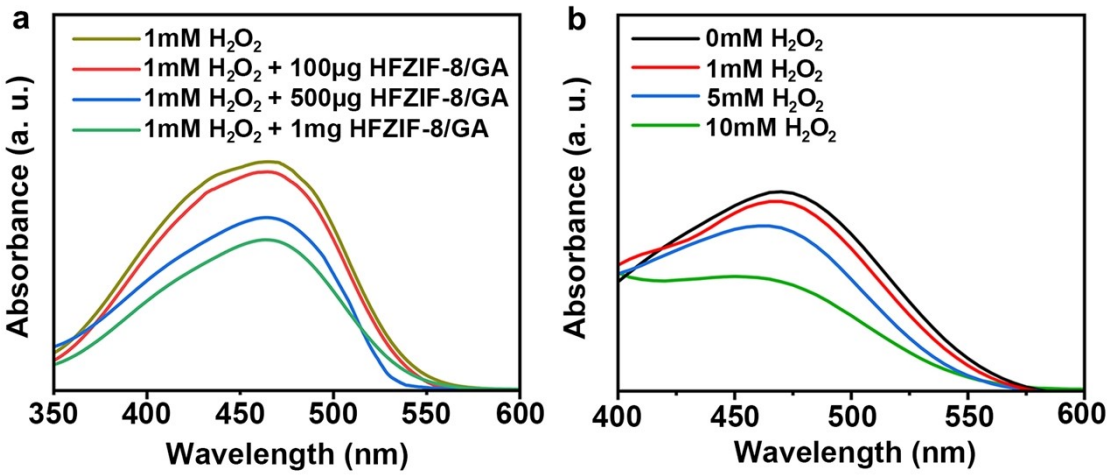

Fig. S13 MO degradation induced by various contents of HFZIF-8/GA plus H_2O_2 (1 mM) (a) and by adding the 500 μg/mL HFZIF-8/GA to various concentrations of H_2O_2 (b) (pH 6.5).

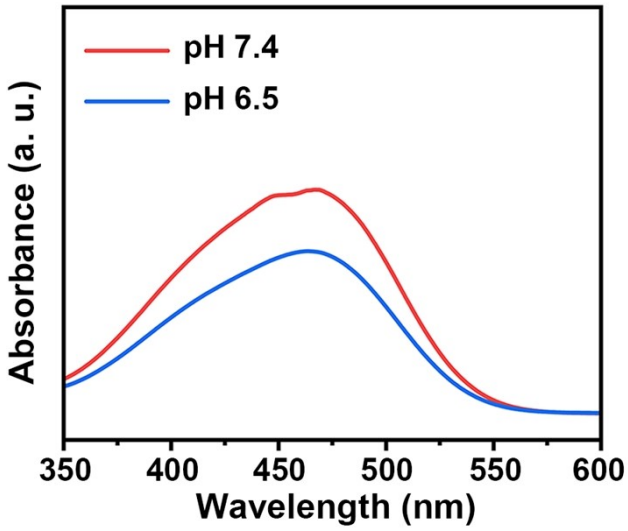

Fig. S14 MO degradations of HFZIF-8/GA under the various conditions plus H_2O_2 (1 mM).

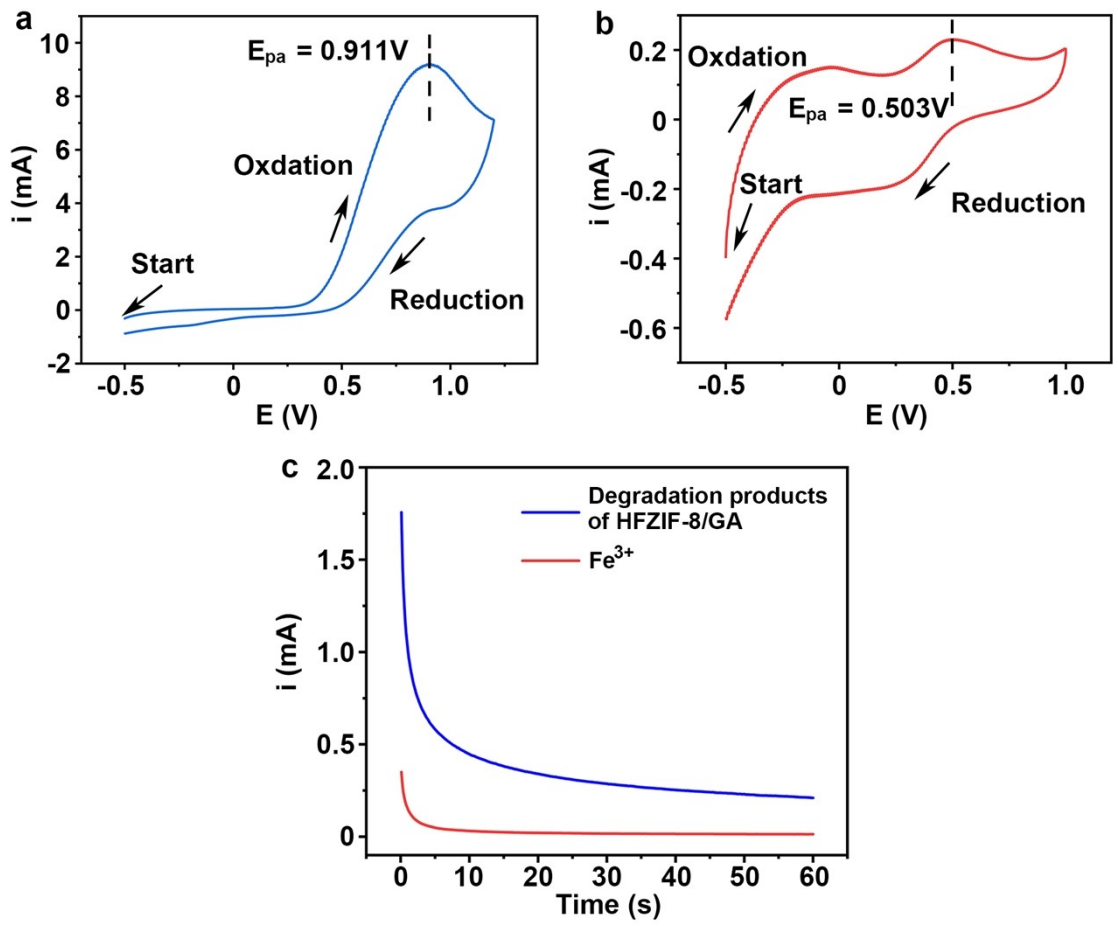

Fig. S15 The CV curve of degradation products of HZIF-8/GA in electrolyte solution (pH 6.5). The CV was originally swept from +1.4 V to -0.5 V. The CV curve investigating redox behavior of fresh Fe^{3+} in electrolyte solution (pH 6.5) (a). The CV was originally swept from +1.0 V to -0.5 V (b). Comparison among limited current responses of electrolyte solutions containing fresh GA-Fe or Fe^{3+} when a half-period of continuous high potential (0.90 V) actions during the successive double potential step transitions of CA (c).

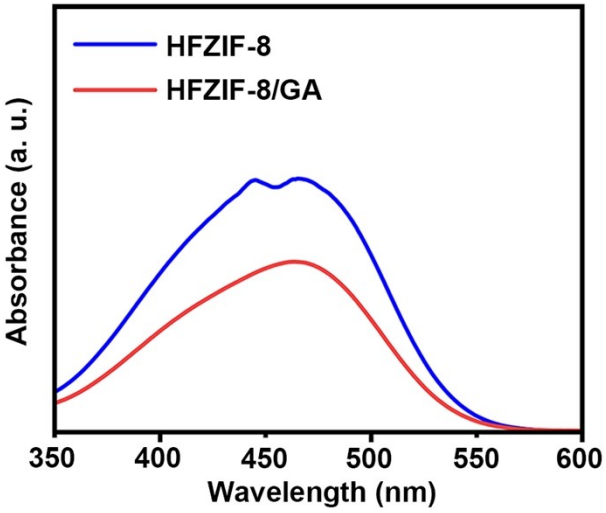

Fig. S16 MO degradation by •OH produced by HZIF-8 and HFZIF-8/GA plus H_2O_2 (1 mM) (pH 5.6).

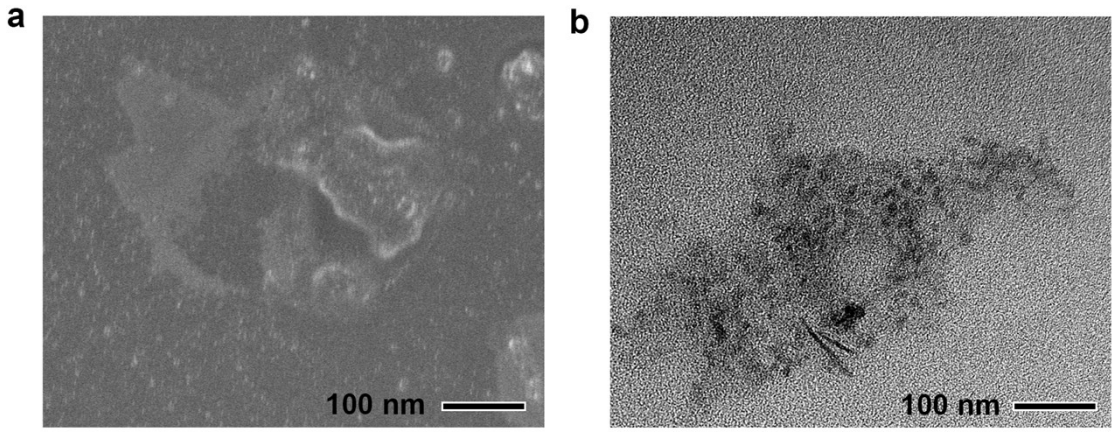

Fig. S17 SEM (a) and TEM (b) images of the HFZIF-8/GA@HA after degradation for 12 h.

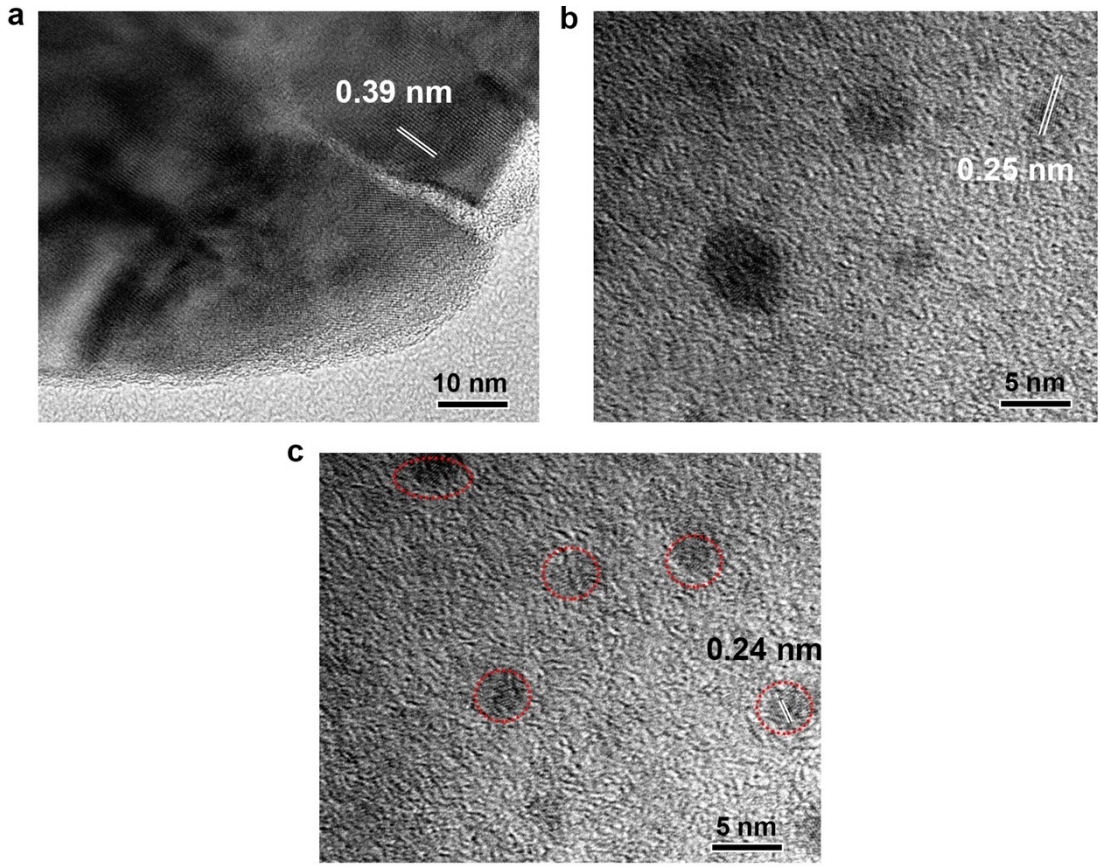

Fig. S18 High resolution TEM images of the Zn-GA (a), Fe-GA(b) and self-assemblies of HFZIF-8/GA@HA after degradation (c).

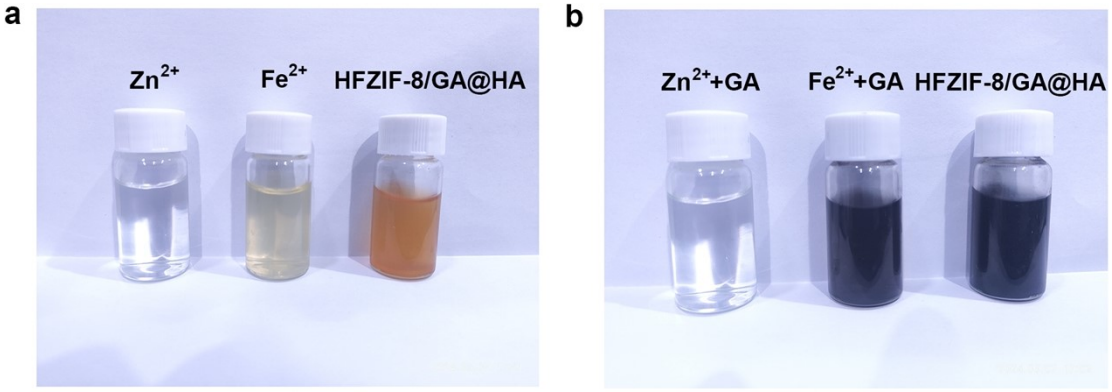

Fig. S19 The photographs of solutions for Zn^{2+} ions, Fe^{2+} ions and HFZIF-8/GA@HA before degradation (a). The photographs of solutions for Zn^{2+} and Fe^{2+} ions with addition of GA as well as HFZIF-8/GA@HA after degradation for 2 h in PBS (pH 6.5) (b).

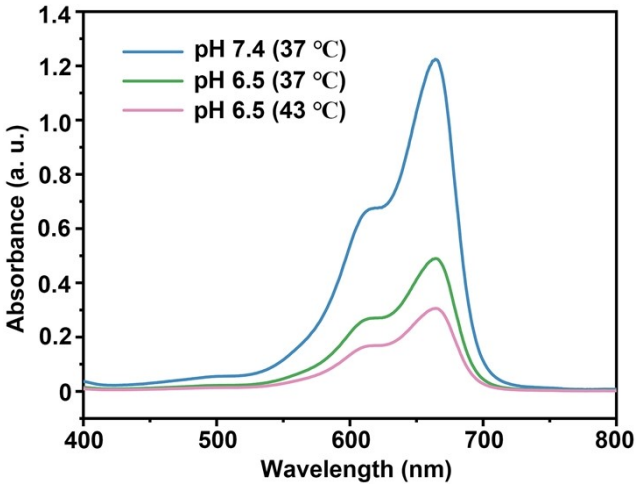

Fig. S20 Detection of ·OH production of HFZIF-8/GA@HA by MB degradation at different conditions.

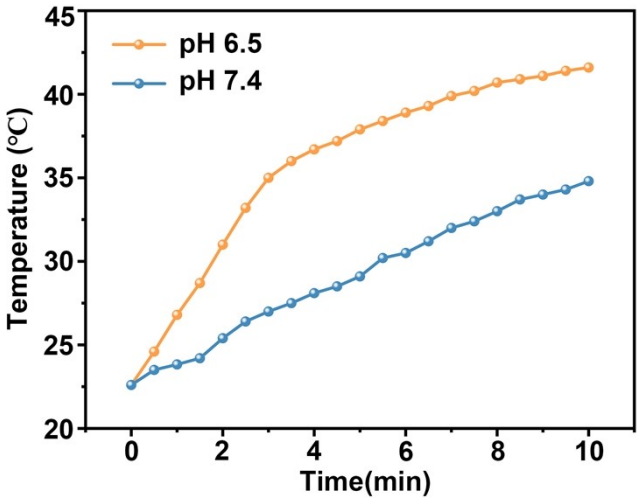

Fig. S21 Temperature change curves of HFZIF-8/GA (500 μg/mL) in different PBS solutions.

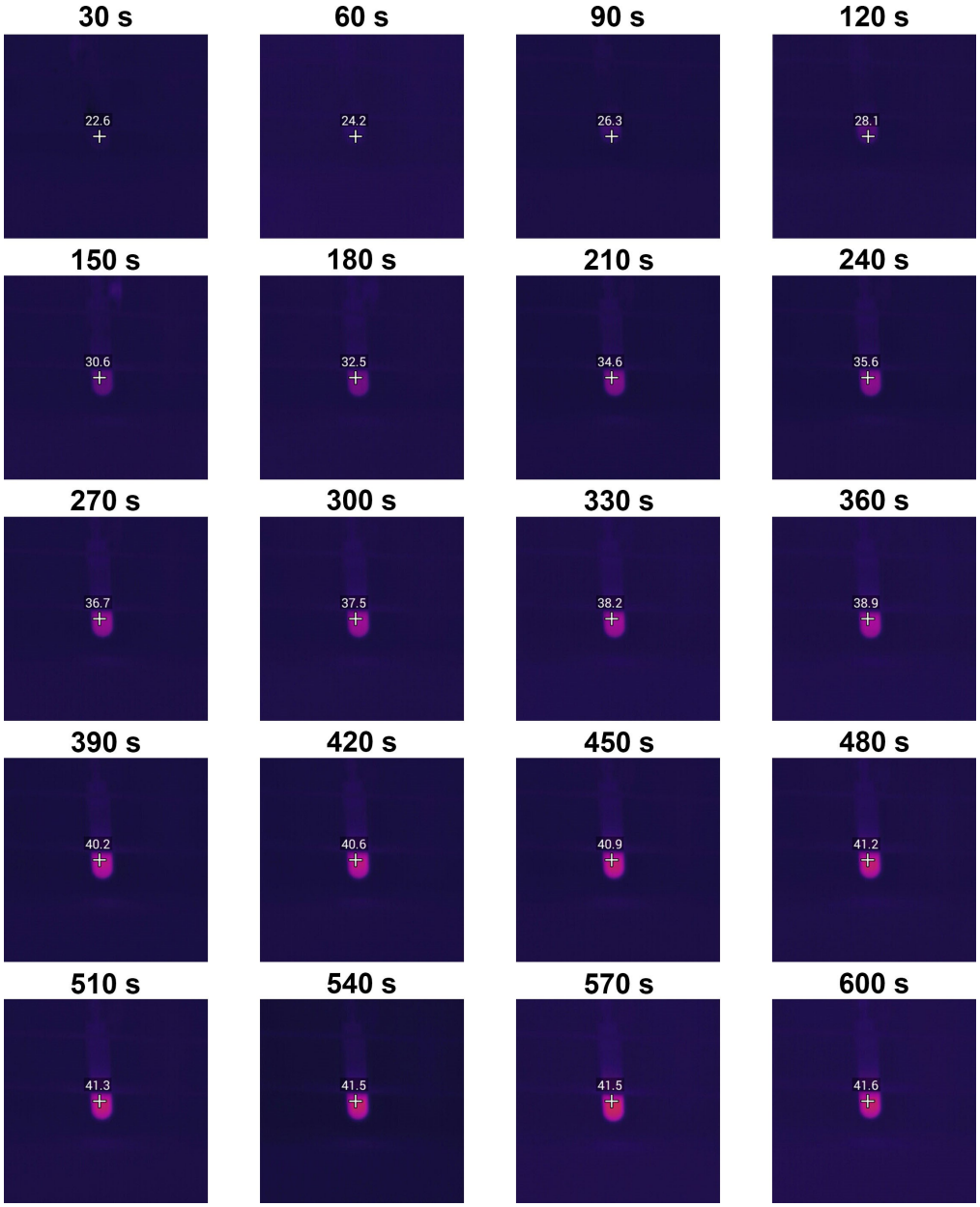

Fig. S22 Photothermal pictures of the degradation products of HFZIF-8/GA dispersed in PBS solution (pH 6.5) under 1064 nm laser (1.0 W/cm^2) irradiation.

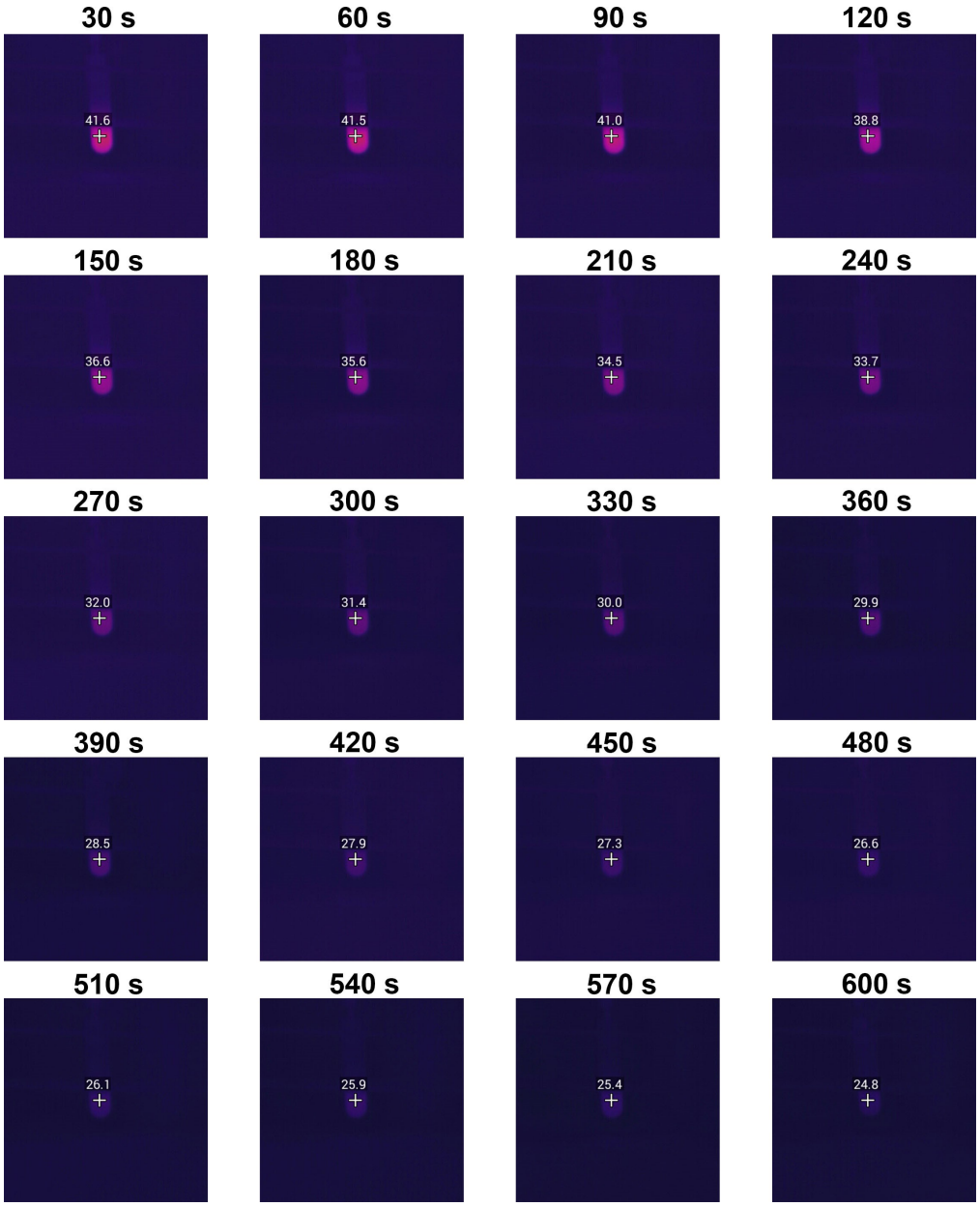

Fig. S23 Photothermal pictures of the degradation products of HFZIF-8/GA dispersed in PBS solution (pH 6.5) after 1064 nm laser turned off.

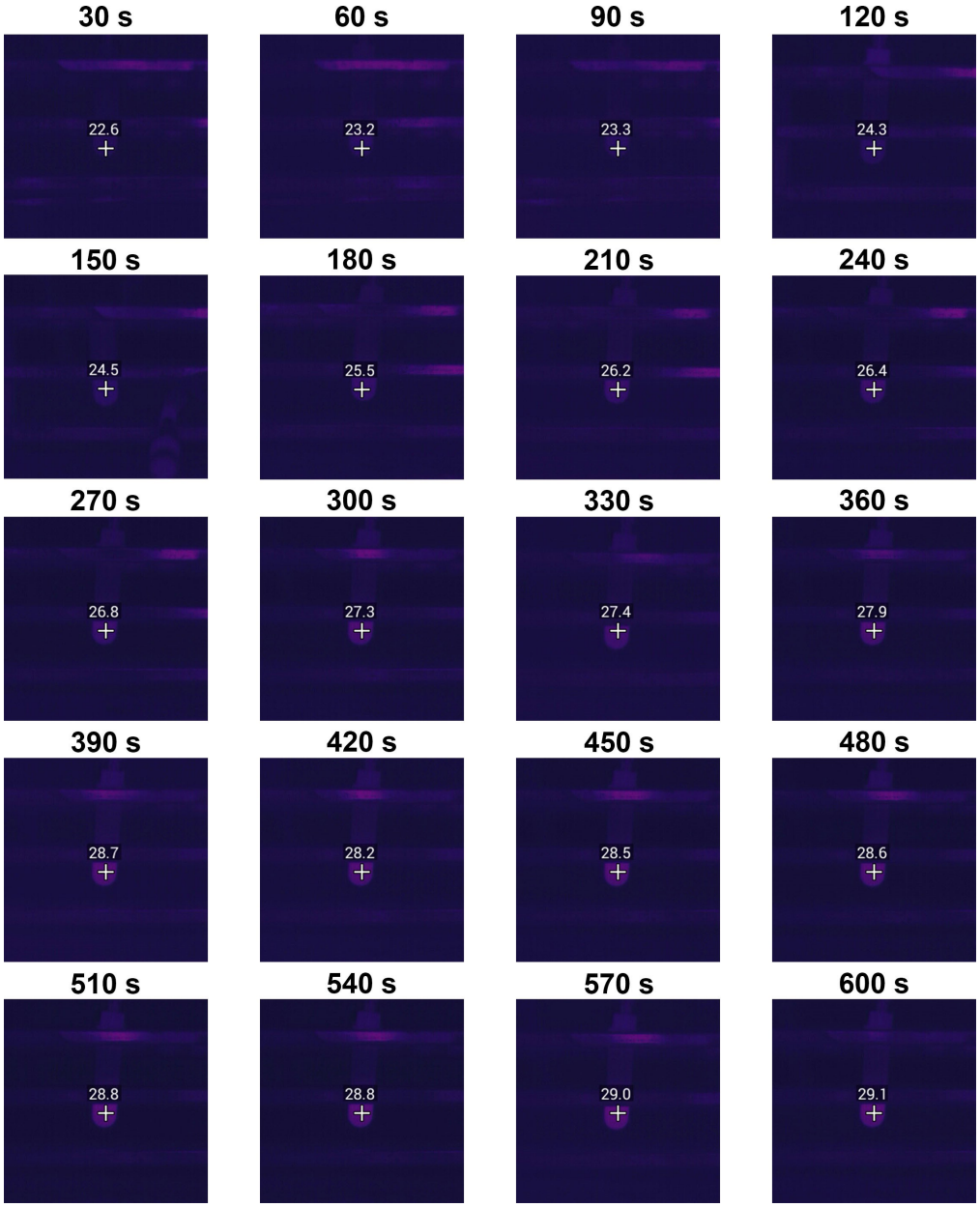

Fig. S24 Photothermal pictures of the deionized water under 1064 nm laser irradiation (1.0 W/cm^{-2}).

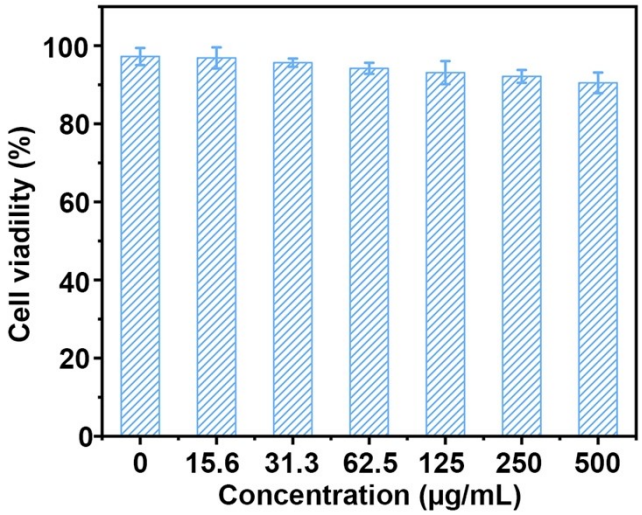

Fig. S25 Cell viabilities of L929 after being incubated with HFZIF-8/GA@HA for 24 h and quantitative assays by standard MTT method.

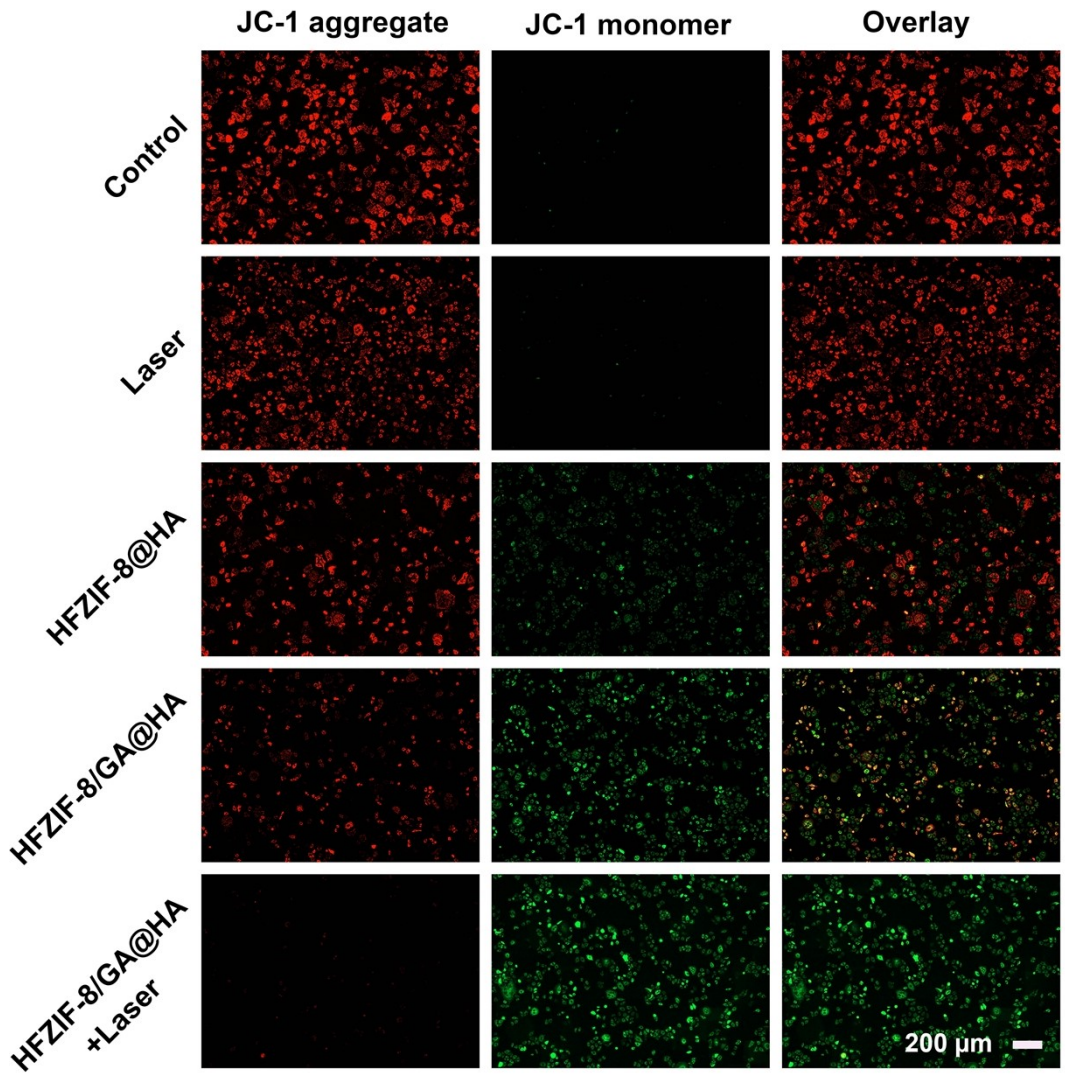

Fig. S26 CLSM images of JC-1-stained HeLa cells in groups of control, 1064 nm laser, HFZIF-8@HA, HFZIF-8/GA@HA and HFZIF-8/GA@HA plus 1064 nm laser.

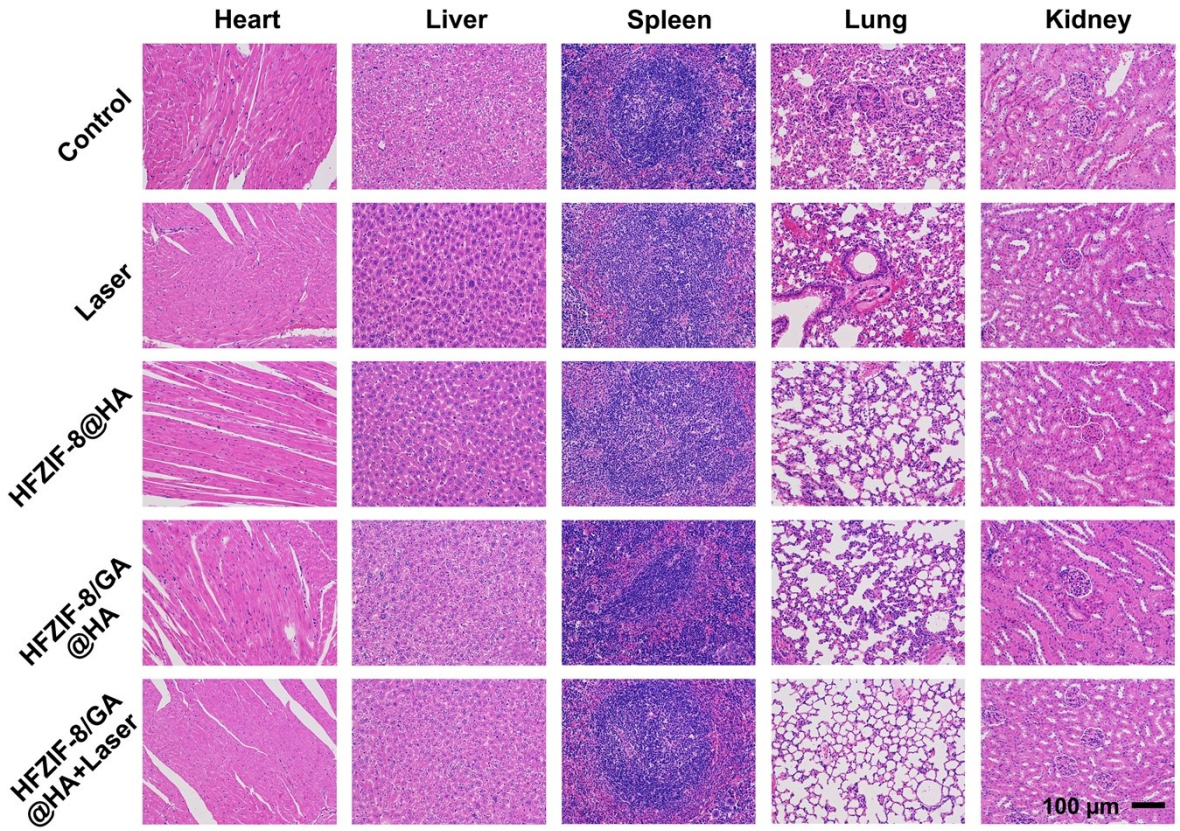

Fig. S27 H&E-stained images of heart, liver, spleen, lung, and kidney in the groups of control, 1064 nm laser, HFZIF-8@HA, HFZIF-8/GA@HA, HFZIF-8/GA@HA plus 1064 nm laser (scale bar: 100 μm).

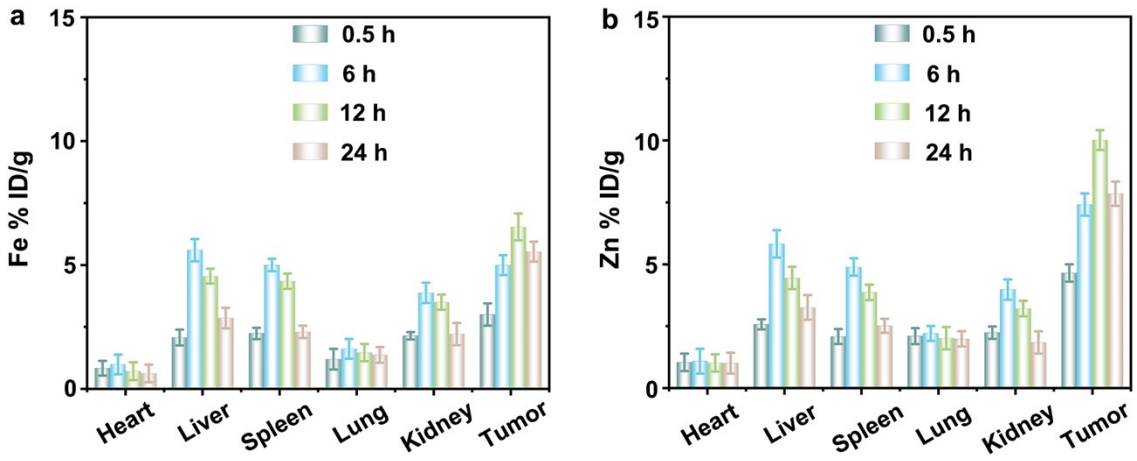

Fig. S28 *In vivo* distribution of Fe (a) and Zn (b) elements in heart, liver, spleen, lung, kidney and tumor tissues of tumor-bearing mice at different time points after tail vein injection of HFZIF-8/GA@HA.

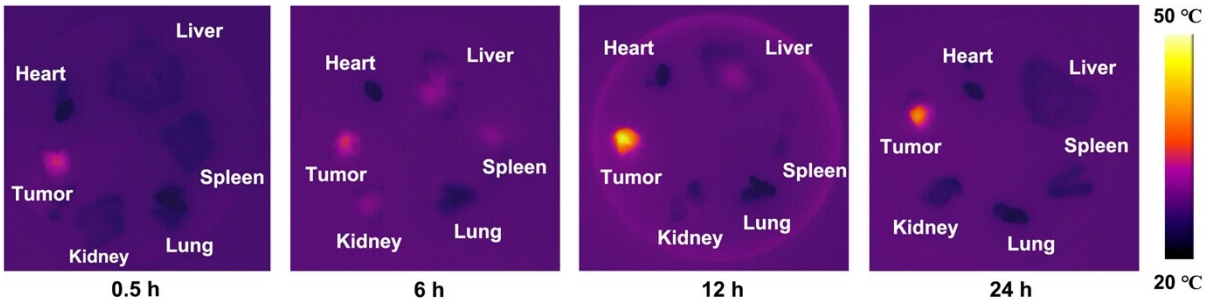

Fig. S29 The thermal images of heart, liver, spleen, lung, kidney and tumor tissues stripped at different time points after tail vein injection of HFZIF-8/GA@HA (1064 nm laser irradiation for 5 min for all the tissues).

Table S1. Blood biochemical assay and hematology analysis for HFZIF-8/GA@HA during treatment on day 0, 1, 7 and 14.

Tests	Units	Treatment (0 day) (mean ± sd)	Treatment (1 day) (mean ± sd)	Treatment (7 day) (mean ± sd)	Treatment (14 day) (mean ± sd)
Biochemistry					
AST	U/L	184.21 ± 16.14	183.16 ± 12.76	182.08 ± 26.14	183.18 ± 17.24
ALT	U/L	59.50 ± 2.30	58.40 ± 3.30	59.10 ± 5.50	58.92 ± 4.40
ALP	U/L	118.12 ± 2.31	119.02 ± 4.63	120.42 ± 4.11	119.02 ± 4.63
BUN	mmol/L	8.65 ± 2.32	8.70 ± 1.32	8.50 ± 2.44	8.70 ± 3.24
TP	g/L	66.50 ± 3.13	64.60 ± 2.34	64.82 ± 4.21	66.96 ± 3.64
Hematological					
WBC	$\times 10^9$/L	6.15 ± 3.35	5.91 ± 2.39	6.02 ± 1.89	6.05 ± 1.95
NE	$\times 10^9$/L	12.80 ± 2.25	11.32 ± 1.62	12.92 ± 3.62	11.72 ± 2.62
LY	$\times 10^9$/L	71.80 ± 2.35	72.25 ± 2.12	73.45 ± 1.62	72.10 ± 1.92
RBC	$\times 10^{12}$/L	8.93 ± 2.37	9.28 ± 2.36	8.85 ± 2.68	9.15 ± 1.96
HGB	g/L	141.21 ± 12.87	142.87 ± 19.33	143.97 ± 15.93	141.78 ± 15.35
MCV	fL	50.50 ± 3.52	48.70 ± 2.14	49.90 ± 2.64	49.50 ± 3.54
MCH	pg	17.30 ± 2.37	17.10 ± 1.22	17.70 ± 3.12	16.50 ± 2.42
MCHC	g/L	361.00 ± 3.25	359.00 ± 4.73	362.00 ± 8.83	357.00 ± 7.93
RDW	%	24.90 ± 2.35	25.20 ± 1.85	25.80 ± 2.75	25.40 ± 4.15
PLT	$\times 10^9$/L	821.21 ± 53.63	819.71 ± 52.74	821.60 ± 52.74	820.63 ± 42.14

Notice: the data in the table is average calculated by five mice each group. Healthy female Kunming mice *i.v.* injected with the composites were sacrificed at 0, 1, 7 and 14 days for blood collection, respectively.